
EFDA–JET–CP(02)04-01

S.J. Cox, A. Bickley, T.T.C. Jones and J. Milnes
and JET EFDA Contributors

Operating Limits of the Upgraded JET Neutral Beam Injector from Duct Re-ionisation and Beam Shine-through

Operating Limits of the Ppgraded JET Neutral Beam Injector from Duct Re-ionisation and Beam Shine-through

S.J.Cox, A.Bickley, T.T.C.Jones and J.Milnes
and JET EFDA Contributors*

EURATOM/UKAEA Fusion Association, Culham Science Centre, Abingdon, OX14 3DB, UK

** See annex of J. Pamela et al, "Overview of Recent JET Results and Future Perspectives",
Fusion Energy 2000 (Proc. 18th Int. Conf. Sorrento, 2000), IAEA, Vienna (2001).*

Preprint of Paper to be submitted for publication in Proceedings of the
19th IEEE/NPSS Symposium on Fusion Engineering
(Atlantic City, New Jersey, USA 22-25 January 2002)

“This document is intended for publication in the open literature. It is made available on the understanding that it may not be further circulated and extracts or references may not be published prior to publication of the original when applicable, or without the consent of the Publications Officer, EFDA, Culham Science Centre, Abingdon, Oxon, OX14 3DB, UK.”

“Enquiries about Copyright and reproduction should be addressed to the Publications Officer, EFDA, Culham Science Centre, Abingdon, Oxon, OX14 3DB, UK.”

ABSTRACT.

Physics modelling and engineering analysis have been carried out to determine the operating limits of the upgraded JET neutral beam injector from duct re-ionisation and beam shine-through. The JET neutral beam duct is only 23cm wide and 90cm tall at its throat and yet it presently has to transmit more than 11MW of D^0 beam particles, resulting in power densities in excess of 200MW/m^2 . Even at this power level, the copper duct liner can be the limiting component with respect to the pulse length of the Octant 4 injector, depending on plasma current and power. The upgrade to the Octant 8 injector in 2002 will increase the power to $\sim 15\text{MW}$ of D^0 at 130kV, so it is necessary to determine the new limits. It is shown that at full power, the duct will become the major limiting component with respect to pulse length for this injector. The shine-through power density and integrated energy for various in-vessel components have also been evaluated for the upgraded injector. Thermo-mechanical finite element stress calculations on elements of the ICRH antenna show that the injector can be operated at full power without further restrictions being imposed on the plasma characteristics, e.g. density and shape. For the CFC inner wall guard limiter tiles and their internal reinforcement, however, there is a bulk temperature limit and an enhancement to the existing real-time protection system is proposed.

I. INTRODUCTION

The upgrade [1] to the JET neutral beam injector at Octant 8 (~ 7.5 to $\sim 15\text{MW}$ of D^0) will be achieved by doubling the injected power per ion source or PINI to $\sim 1.9\text{MW}$. Previous assessments of the beam duct and in-vessel components were made using a maximum nominal power of 1.7MW/PINI for the Octant 4 injector. Therefore, a re-assessment of the limits of these components is required and is the subject of this work.

Figure 1 shows the layout of the neutral beam injectors at JET and the points of interaction of the beams with the JET vessel. Upstream of the duct, the pressure in the beam-line is minimised by the use of large cryopumps that line the walls of the neutral injector boxes or NIBs. Nevertheless, there is still significant re-ionisation of the neutral beam ($\sim 2\%$) due to collisions with gas molecules. These ions are ‘collected’ in the beam in this low magnetic field region. As the beams enter the duct, the ions are influenced by the stray magnetic fields from the tokamak which cause them to be deflected and focused onto the walls. In addition, a small fraction of the neutral beam ($\sim 5\%$) is directly intercepted by the duct protection, although the power density tends to be lower as there is no focusing action for these particles. The bombardment of the walls by energetic particles leads to gas re-emission that appears to be temperature related. This desorbed gas increases re-ionisation in the beam path leading to higher power loading on the walls, higher temperatures and increased desorption. In extreme circumstances, this feedback mechanism can block the beam propagation entirely [2].

A water-cooled copper liner protects the duct, and the derivation and implementation of the operational limits of this component are discussed in Section II. In order to establish the duct gas evolution characteristics, a pressure balance model [3] has been used to derive a beam particle induced gas re-emission coefficient from the present duct pressure data. Section III shows how this is done and how the data is scaled to the higher power levels of the upgrade scenario in order

to derive new operational limits.

After the duct, the neutral beams enter the torus and are attenuated by the JET plasma depending on the plasma characteristics, e.g. density and shape. The neutral beams follow either ‘normal’ or ‘tangential’ trajectories as shown in Fig.1. The transmitted or shine-through power from ‘normal’ beams falls on the inner wall of the torus, whereas the ‘tangential’ beams strike the outer wall after passing through the plasma for a second time. The effect of this power density on components at these locations is given in Section IV. Section V summarises the results of these assessments.

2. DUCT PROTECTION

The present duct liners were installed in 1993 and additional radiation cooled tiles were added in 1995 to allow operation at lower plasma currents. Applying limits to the operation of the injectors protects the duct liners:

2.1. TEMPERATURE LIMIT

The surface temperature rise of the liner is restricted to 500°C in order to limit crack propagation. The re-ionised power focus does not always fall on the thermocouples buried in the copper, so protection is achieved by applying pulse length limits, t_{500} , to the injector. These are derived as follows:

- A 3D ion tracking code [4] is benchmarked against thermocouple data in order to derive certain model parameters, e.g. a constant duct pressure of 2×10^{-5} mbar.
- These parameters are then used to predict the re-ionised power density in other plasma configurations.
- The total power density, $\langle PD \rangle$, is obtained by adding the directly intercepted component (derived from thermo-couples in ‘counter’ injection shots, where the re-ionised power density is lower than in ‘co’ injection) to the re-ionised component averaged over an area of 25cm^2 .
- The thickness of the copper liner at the focus is used in a 1D heat diffusion model in order to predict the time for the surface temperature of the copper to rise by 500°C.

For the present Octant 8 injector, t_{500} is greater than ten seconds (the standard injector pulse length limit) for all the plasma configurations studied. On the other hand, the Octant 4 injector at 1.4MW/PINI can have values less than ten seconds depending on the plasma current, I_p , as shown in Table I. In these circumstances, the duct becomes the limiting component with respect to beam pulse length.

I_p (MA)	Depth of Cu at focus (cm)	$\langle PD \rangle$ (W/cm ²)	t_{500} (s)
1	2	430	6.90
1.5	3	385	10.9
2	3.5	360	13.3
2.5	4	370	14.1
3	4-4.5	415	12.5
4	4.5	440	11.9
5	4	470	10.1

TABLE I: t_{500} for the Octant 4 injector at 1.4MW/PINI.

2.2. PRESSURE LIMIT

Simplistically, one would expect the duct pressure to reach an equilibrium where the gas flux desorbed from the walls equals the incident particle flux. This is what is assumed in the analysis of the temperature limit. However, the feedback mechanism described in Section I can lead to an increasing duct pressure as shown in Fig.2. The beams come on at $t=0$ and the pressure rises rapidly to a quasi-equilibrium. Then there is a slower rise over a period of a few seconds that is thought to be due to an increase in wall temperature from the particle bombardment. There is no active cooling of the liner during the beam pulse, so the copper at the power focus can reach temperatures of several hundred °C. Gas release from a metal is complicated but there are thermal processes that tend to dominate at high temperature, such as diffusion and re-combination [5]. As the pressure rises, the re-ionised power increases, so a pressure limit has to be set. This was derived empirically in 1995 at 3.1×10^{-5} mbar and is implemented through the Fast Beam Interlock System, FBIS [6,7]. These limits appear to be effective in protecting both duct liners as no damage has been seen since installation. The benchmarking described earlier shows that a duct pressure of 2×10^{-5} mbar describes the present injectors well. For the upgrade, however, we expect an increase in pressure as the injected neutral flux will approximately double. A model is required to predict the duct pressure before an assessment of the new limits can be made.

3. THE DUCT PRESSURE MODEL

A semi-empirical model [3] has been used to analyse the duct pressure, P , for the present injectors in terms of a gas re-emission coefficient, Γ , equal to the number of molecules released from the duct wall per incident ion or atom. Under ideal equilibrium conditions, $\Gamma = 0.5$, however, values as high as 33 have been obtained for an unconditioned duct on the first beam pulse [3]. There are a number of gas sources that contribute to the pressure in the duct: the residual of the NIB gas flow that enters the duct, Q_0 , the re-emission from the directly intercepted atoms, Q_d , and the re-emission from the re-ionised ions, Q_w . If Γ varies only slowly over a pulse then the solution to the pressure balance equation is,

$$P = \left(P_0 - \frac{\tau' Q}{V} \right) \exp \left(-\frac{t}{\tau'} \right) + \frac{\tau' Q}{V} \quad (1)$$

where P_0 is the pressure before the beams come on, $Q=Q_0+Q_d$ and V is the volume of the duct. The vacuum time constant of the duct, τ' , is given as,

$$\tau' = \frac{V}{C - \sigma_{01} L \phi_B \Gamma} \quad (2)$$

where C is the conductance for gas released in the duct, σ_{01} is the cross-section for re-ionisation, L is the duct length and ϕ_B is the neutral flux entering the duct. This analysis assumes that the gas in the duct is at 300K. Each source of gas derives from different locations and so will have a different

characteristic temperature. In practice, the gas accommodates rapidly to the average wall temperature and so the assumption of 300K should be reasonable. By using a linear variation of the form $\Gamma = mt+c$, where m and c are constants, the predicted pressure can be fitted rather well to the real pressure as shown in Fig.2.

A number of shots from the experimental campaigns in 1999 and 2000 have been analysed with the method outlined above. These data were selected using the following criteria: approximately constant beam power, long pulse lengths, low torus gas flow and similar PINI turn on times. This limits the database but the re-emission coefficient values for the Octant 8 injector are shown in Fig.3 as a function of injected power. The data points indicate the values of Γ at beam turn on, Γ_0 , and the bars indicate the time evolution of Γ over a ten second beam pulse. The increase in Γ_0 with power was not expected and no physical basis can be identified for this effect (a similar analysis on the Octant 4 injector shows a decrease in Γ_0 with power). It appears as though the initial pressure rise after the beam turn on is not modeled correctly. This is not surprising as the model assumes that gas is re-emitted instantaneously whereas in reality, there is a complicated time response [5]. As a compromise, $\Gamma_0 = 0.5$ is used for extrapolations to the upgrade. Nevertheless, the final value of Γ increases with power as expected, indicating out-gassing in excess of the deposition rate. It also extrapolates to ~ 0.5 at zero power, the expected minimum value of Γ under ideal equilibrium conditions, which gives some confidence in the model.

The power scalings for Γ from both injectors can be used to extrapolate to the Octant 8 upgrade power of $\sim 15\text{MW}$, although the scaling from the Octant 8 injector data is more relevant as it was taken at almost the correct beam energy. The pressure balance model, Equation 1, can now be used to predict the duct pressure. The re-ionised power focus for the upgrade is assumed to be the same in terms of shape and location as that for the present Octant 8 injector. The new values of t_{500} can now be calculated as follows:

- The directly intercepted power density is scaled by the increase in power due to the upgrade (this assumes that the directly intercepted fraction is unchanged).
- The averaged re-ionised power density is scaled by the power increase *and* by the increase in the re-ionised fraction, $\sim \sigma_{01} n L$ where n is the predicted gas density.
- The combined power density variation with time is used in a 1D heat diffusion model in order to predict t_{500} .

The result of this analysis is that at 15MW, the duct surface temperature rise will reach 500°C after only **5 to 6 seconds** of beam. The range derives from the use of the Γ power scalings from the two injectors, i.e. whichever scaling is used has little effect. This time limit would allow some experiments in the optimised shear, OS, plasma regime but would restrict the development of the steady-state OS and ELMy H-mode scenarios. Experiments at high torus gas flow, such as those at the Greenwald density, are known to influence the duct pressure. Therefore, less than five seconds should be anticipated for these shots. In tritium, t_{500} will be even shorter due to the increase in power. It can

be predicted that the duct will become the major limiting component with respect to pulse length for the upgraded injector.

The time limits could be increased by reducing the injector power or by allowing the wall temperature to rise by more than 500°C. More complicated solutions can be envisaged such as increasing the duct pumping speed or re-designing the liners.

4. SHINE-THROUGH

The effect of the upgraded shine-through power on various in-vessel components has been assessed in the following way:

- The unattenuated power density profiles for the upgraded PINIs at the points of interest are calculated using a beam transmission code.
- The shine-through fraction for each PINI is calculated using a beam deposition code which integrates the plasma density along any line-of-sight. For this assessment, the plasma characteristics at the present operating limits were used, e.g. minimum line-integrated density.
- The power density profiles are modified by the shine-through fraction and are then overlaid onto the in-vessel components using the JET drawing office CATIA system.

Even with the upgraded PINIs, the power density remains below the prescribed limits ($<50\text{W}/\text{cm}^2$ on the vessel wall and $<100\text{W}/\text{cm}^2$ on other inconel structures) at the present plasma operating limits. This is due to the improved accuracy of this present assessment, however, there are two additional issues:

4.1. ICRH ANTENNA

Thermo-mechanical finite element analyses have been carried out on the components of the ICRH antenna, and the highest risk is to a nimonic bolt (part of the beryllium Faraday screen bars) as shown in Fig.4. A significant surface temperature rise to ~70% of the melting point is seen for a ten second beam pulse, assuming no cooling by conduction or radiation.

4.2. INNER WALL GUARD LIMITER

The profiles from two 'normal' PINIs overlap on the inner wall guard limiter as shown in Fig.5. At the plasma operating limits, the power density will be $\sim 17\text{MW}/\text{m}^2$ normal to the surface of the central CFC tile. Modelling has shown that after ten seconds of plasma followed by approximately one second of beam injection, the bulk temperature of the tile will exceed the inconel yield limit of the tile's internal tie-rod (700°C). In practice, however, the plasma density rarely remains at the operating limit due the fuelling effect of the beams.

Both of these issues can be addressed by a modification to JET's real time protection system, i.e. to compute the temperature of a particular component in real time. Look-up tables will be used to obtain the peak shine-through power density, S_{max} , for each PINI from the line-integrated plasma density. The table used will depend on parameters such as the beam species and the plasma shape.

A further parameter is needed to relate each value of S_{\max} to the power density normal to the surface of each affected component. Finally, a transfer function is applied depending on the temperature response of the component at risk. This is equivalent to a convolution integral of the power density to obtain the temperature. If the response function is not constant with power density, then a second look-up table is required to hold these values. If the component limit is exceeded, then the corresponding beam permit will be removed from FBIS.

CONCLUSIONS

The analysis reported here predicts that a five to six second, 15MW beam pulse from the Octant 8 upgraded injector will increase the surface temperature of the copper duct liner by 500°C. This will restrict JET's experimental programme, particularly if high densities and long pulses are required. Therefore, it is recommended that the engineering limit of 500°C be re-examined. In the longer term, it may be possible to increase the pumping in the duct region and to re-design the duct liner, although this will require in-vessel access. In terms of shine-through, the injector can be operated at full power without further restrictions being imposed on the plasma characteristics. However, a modification to the real time protection system is required in order to assess the bulk temperature of the CFC inner wall guard limiter tiles.

ACKNOWLEDGEMENTS

We would like to acknowledge H. deEsch (CEA, Cadarache) for the development of the 3D ion tracking code on which this paper is based. This work has been conducted under the European Fusion Development Agreement and is partly funded by Euratom and the UK Department of Trade and Industry.

REFERENCES

- [1]. D. Ciric et al, these proceedings.
- [2]. A. Riviere et al, *Nuc. Fus.* **15**, 944-947 (1975).
- [3]. A. Bickley et al, 13th IEEE Symposium on Fusion Engineering, (1989).
- [4]. H. deEsch et al, 16th Symposium on Fusion Technology, London, (1990).
- [5]. G. McCracken et al, *Nuc. Fus.* **19**, 889-981 (1979).
- [6]. D. Cooper et al, 12th Symposium on Fusion Engineering, Monterey, (1987), pp.1096-1100.
- [7]. D. Stork et al, *Fus. Eng. & Des.* **47**, 131-173 (1999).

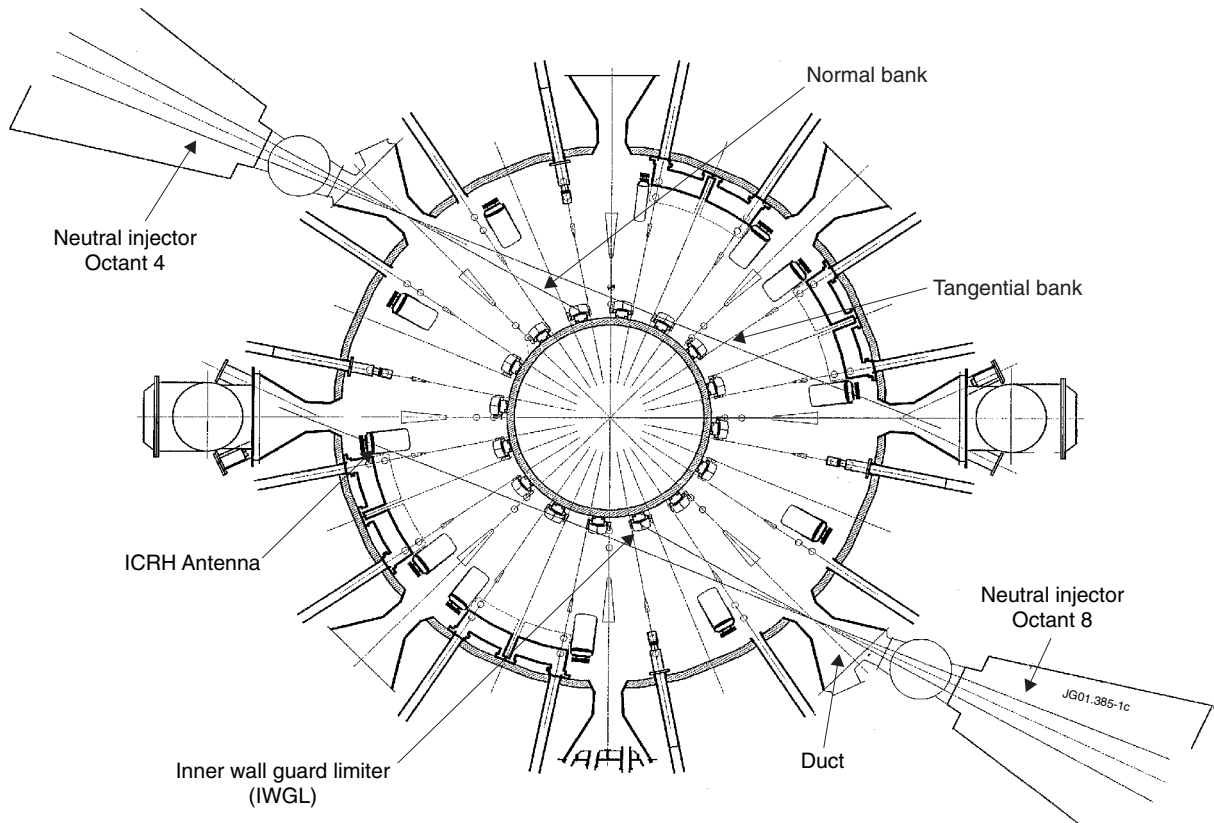


Figure 1: The neutral beam injectors at JET.

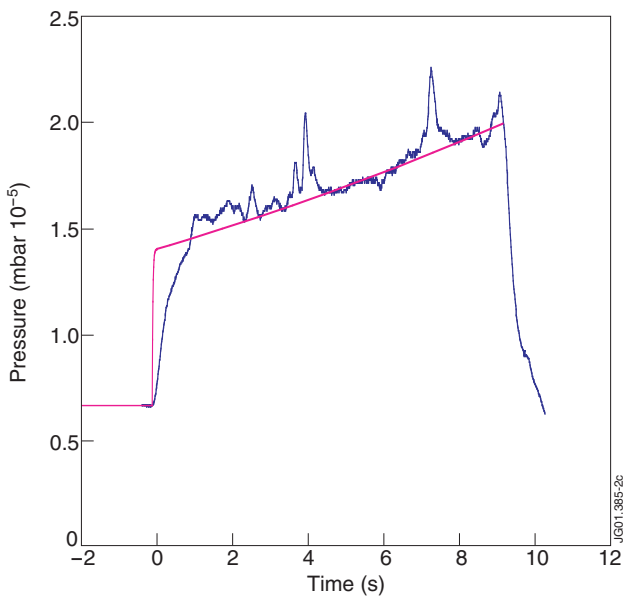


Figure 2: A typical duct pressure waveform and the predictions of the pressure model.

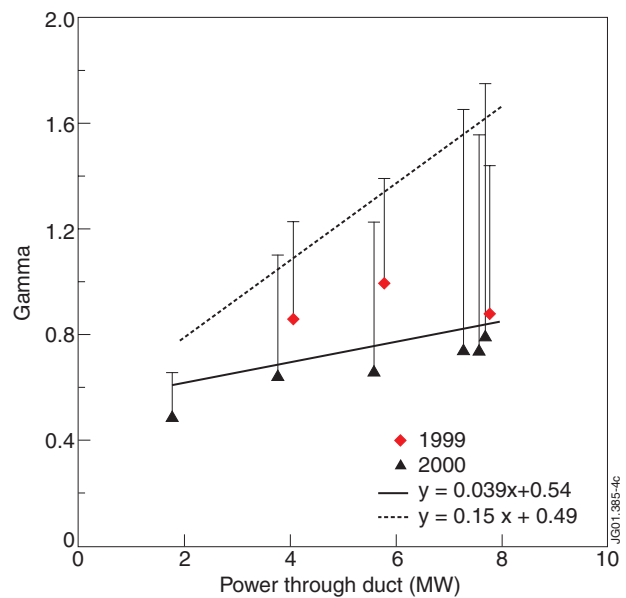


Figure 3: Re-emission coefficient values for the Octant 8 injector.

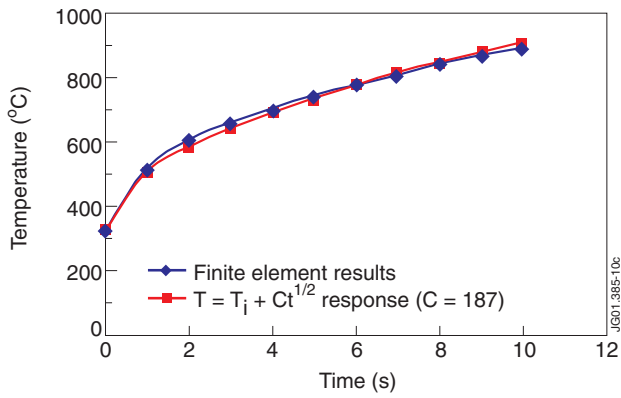
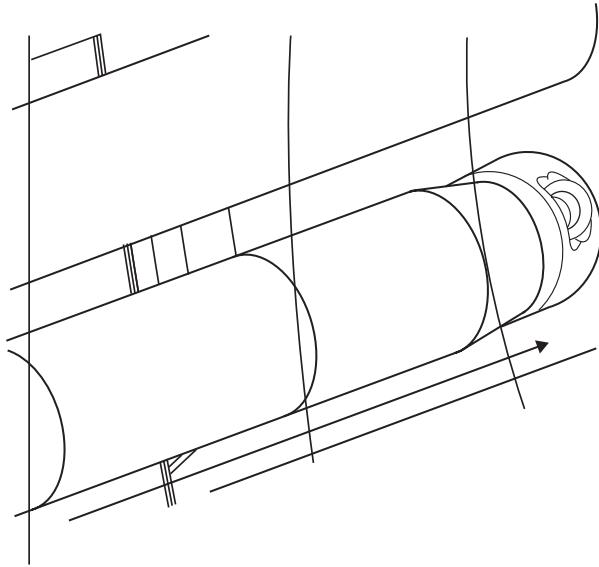


Figure 4: The nimonic bolt and its temperature response.

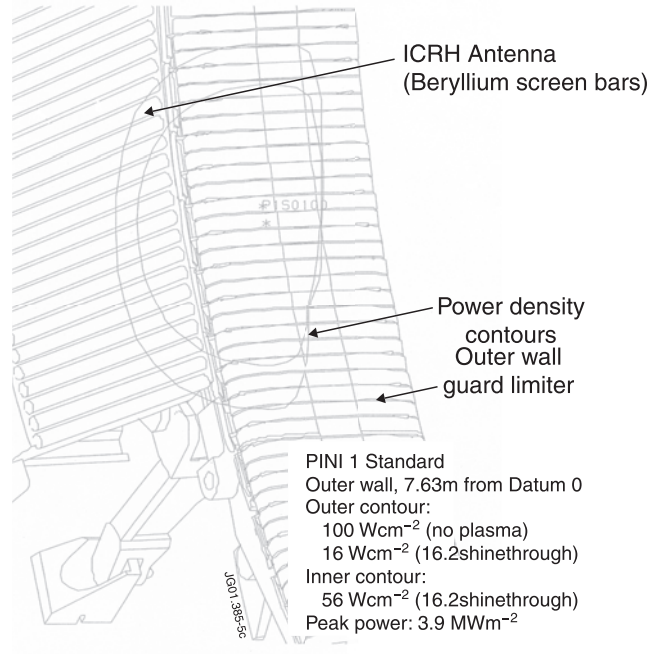


Figure 5: The shine-through profile on the inner wall.